4f-5d Transitions of Tb3+ in Cs2NaYF6: The Effect of Distortion of the Excited-State Configuration

4 AUTHORS, INCLUDING:

Chang-Kui Duan
University of Science and Technology of China
177 PUBLICATIONS   1,811 CITATIONS

SEE PROFILE

Peter Anthony Tanner
The Hong Kong Institute of Education
355 PUBLICATIONS   4,367 CITATIONS

SEE PROFILE

Andries Meijerink
Utrecht University
364 PUBLICATIONS   13,485 CITATIONS

SEE PROFILE

4f−5d Transitions of Tb³⁺ in Cs₂NaYF₆: The Effect of Distortion of the Excited-State Configuration

Chang-Kui Duan,[†,‡] Peter A. Tanner,[*,†] Andries Meijerink,[§] and Vladimir Makhov[∥]

[†]Department of Biology and Chemistry, City University of Hong Kong, Tat Chee Avenue, Kowloon, Hong Kong SAR, People's Republic of China

[‡]Department of Physics, The University of Science and Technology of China, Hefei, Anhui, People's Republic of China

[§]Debye Institute, Department of Chemistry, Utrecht University, Princetonplein 5, 3584 CC Utrecht, The Netherlands

[∥]P. N. Lebedev Physical Institute, Leninskii Prospect 53, 119991 Moscow, Russia

ABSTRACT: The low-temperature absorption and excitation spectra of interconfigurational 4f−5d transitions of Tb³⁺ in a cubic fluoride host demonstrate the appearance of a first-order linear Jahn−Teller effect for the high-spin excited states of the excited electronic configuration 4f⁷5d involving 5d t_{2g} orbitals. The τ_{2g} mode is observed to be responsible for the splitting of the otherwise degenerate 5d t_{2g} orbitals.
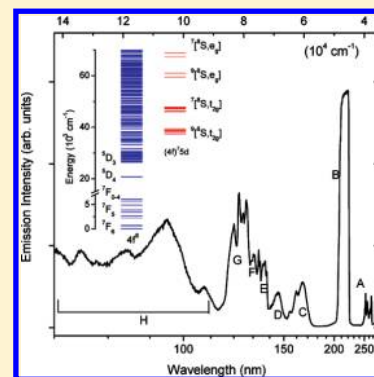
INTRODUCTION

The 4f^N energy levels of lanthanide ions, Ln³⁺, have been well-simulated[1] and exploited in optical devices such as lasers, phosphors, and fiber optics, with newer applications in bioimaging and upconversion. More recently, attention has focused upon the higher energy configuration, 4f^{N−1}5d, which has been probed with the use of synchrotron radiation. Thus, the 4f^{N−1}5d energy levels and 4f^N−4f^{N−1}5d transition intensities of Ln³⁺ have been intensively studied in wide band gap host lattices, especially fluorides and phosphates. The theoretical outcome has been an extension of the conventional 4f^N semiempirical model to incorporate an outer d-electron, with inclusion of the crystal field and spin−orbit coupling, as well as the interaction of the d-electron with the 4f^{N−1} core.[2−5] The theory thus enabled an understanding of the vacuum ultraviolet (vacuum-UV) excitation spectra, as well as the 4f^{N−1}5d → 4f^N emission spectra and luminescence lifetimes. The simplest excitation spectrum, that of Ce³⁺, exhibits up to five bands in low-symmetry hosts, which denote the crystal field splitting of the d-electron states. In the cubic host lattice CaF₂, the orbital d-electron states split into t_{2g} and e_g, with the former at higher energy since the electrons are directed toward fluoride ligands. However, the elpasolite host lattice, Cs₂NaYF₆, gives the opposite ordering of these orbital states because the Ln³⁺ is situated at an octahedral site. With respect to spin states, the coupling of d- and f-electrons for the ions in the second half of the lanthanide series 4f^N (N > 7) gives rise to 4f^{N−1}5d high-spin (HS) and low-spin (LS) states, as shown schematically in the insert of Figure 1(a) for Tb³⁺, which

have markedly different transition intensities from the electronic ground state. For this ion, 4f⁸ Tb³⁺, since the electronic ground state is ⁷F₆ (S = 3), the spin-forbidden (SF) transitions to lower energy HS (S = 4) states are much weaker than to the LS (S = 3) states.

From the analyses of the vacuum-UV excitation spectra of this ion in the host lattices CaF₂, YPO₄, and LiYF₄, it was concluded that the 4f^{N−1} core states and the 5d crystal field levels are not strongly coupled.[6] Qualitatively, the spectra almost provided a superposition of the uncoupled 4f^{N−1} and 5d crystal field energy levels, without vibronic structure. Interestingly, the transitions involving the upper d-electron t_{2g} states were lifetime-broadened, whereas those to the lower e_g states were not.[4] More recently, ab initio calculations have provided an added impetus to 4f^N → 4f^{N−1}5d studies through the understanding of the changes in bond length and breathing mode vibrational frequencies upon excitation.[7,8]

The elpasolite lattice confers high energy level degeneracy and strict transition rules at the O_h site for Ln³⁺ doped into this host. Thus the 4f⁸ → 4f⁷5d absorption spectrum of Tb³⁺ in Cs₂NaYCl₆ is considerably simplified so that only three electronic transitions are allowed at low temperature in the lower energy SF spectral region. The observed spectrum is therefore uncluttered, and vibrational progressions in totally symmetric modes
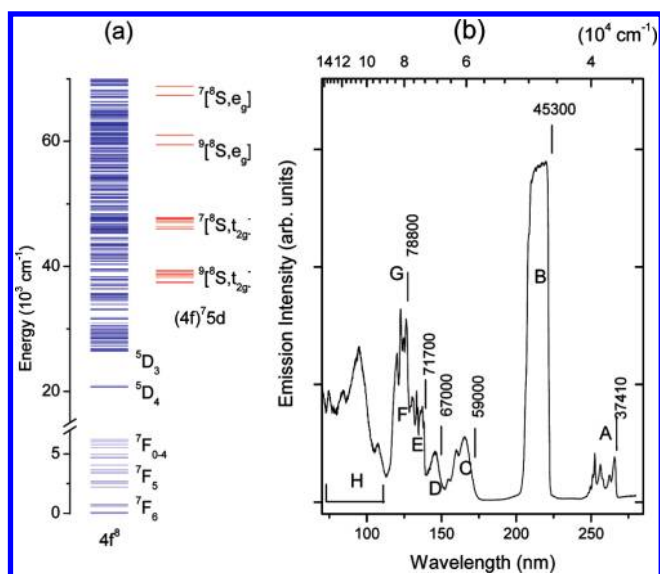
Figure 1. Schematic illustration of the $4f^8$ crystal field states, high-spin $(2S + 1 = 9)$ and low-spin $(2S + 1 = 7)$ states of the $4f^7 5d^1$ configuration (a) and the excitation spectrum of $Cs_2NaY_{0.9}Tb_{0.01}F_6$ detected by monitoring the $^5D_4 \rightarrow {}^7F_5$ emission at 541 nm at 12.6 K (b). The vertical lines are indicative of the zero-phonon lines of the absorption bands.

are well-resolved.[9] We recently reported an overview of the vacuum-UV spectra, together with spectral simulations for various lanthanide ions doped in the analogous cubic Cs_2NaYF_6 host.[5,10] These studies are extended herein with an in-depth analysis of the spin-allowed (SA) and SF transitions of Tb^{3+} in this host.

We report herein a distortion for the states of the $4f^7 5d$ excited configuration of Tb^{3+} and discuss its origin. The d-electron states are labeled $^{2S'+1}[(4f^7$ core $^{2S+1}L_J)5d]$, where the outer $2S'+1$ label denotes the overall spin multiplicity (in this case, 7 or 9 for Tb^{3+}); the $4f^7$ core is labeled by the dominant Russell—Saunders multiplet term; and the 5d electron orbital state is t_{2g} or e_g.

■ EXPERIMENTAL SECTION

The synthesis of materials and the experimental details have been summarized elsewhere.[5,9,10] Low-temperature excitation spectra were recorded for different crystals of $Cs_2NaY_{0.99}Tb_{0.01}F_6$ by two different research groups at the HIGITI station of the DESY synchrotron. The absorption spectrum was recorded for a crystal of $Cs_2NaY_{0.9}Tb_{0.1}F_6$ at higher resolution at CityU using a xenon lamp, an Acton 0.5 m monochromator, and a back-illuminated SpectruMM CCD detector. The sample was housed in an Oxford Instruments Optistat CF continuous flow top loading static cryostat.

■ RESULTS AND DISCUSSION

From the extensive two-photon excitation studies of the $4f^8$ energy levels in the Cs_2NaTbF_6 system,[11] and from our $4f^8 - 4f^8$ intraconfigurational electronic spectra, it is clear that the cubic structure is retained at helium temperature,[11] so that Tb^{3+} occupies a site of octahedral symmetry. This behavior contrasts with the phase transitions in some other hexafluoroelpasolites, which are associated with lattice instability due to rotation of LnF_6^{3-} ions, caused by phonon-mode condensation.

The 12.6 K excitation spectrum of $Cs_2NaY_{0.99}Tb_{0.01}F_6$ in the region from 70 to 280 nm is shown in Figure 1(b). In crystals

doped with Ln^{3+}, the interconfigurational $4f^N \rightarrow 4f^{N-1}5d$ electronic transitions are electric dipole (ED) allowed, subject to SLJ selection rules, and certain point group selection rules which are subsequently mentioned. Following van Pieterson et al.,[2] the sharp bands labeled A, B, E, F, and G are due to transitions from $4f^8$ $^7F_6$ to $4f^7(5d\ t_{2g})$ states and broad bands are due to transitions from $4f^8$ $^7F_6$ to $4f^7(5d\ e_g)$ states. Bands denoted by H are due to host absorption since they appear also in the excitation spectra of Cs_2NaYF_6 doped with other Ln^{3+} ions. The saturated band B is the characteristic $4f \rightarrow 5d$ SA transition to terminal states $^7[(4f^7\ ^8S)\ t_{2g}]$, whereas the weaker, structured bands A are assigned to $4f \rightarrow 5d$ SF transitions to terminal states $^9[(4f^7\ ^8S)\ t_{2g}]$. We note the superscripted numbers 7 and 9 before the square brackets represent $2S + 1$, where S is the total spin of $4f^7 5d$ states. The splitting between A and B, $\Delta E(LS-HS) = \sim 7900\ cm^{-1}$, is due to exchange interaction between 4f and 5d electrons. Theoretically,

$$
\begin{aligned}
H_{ex}(fd) &= -J_{ex}\mathbf{S}_f \cdot \mathbf{S}_d \\
&= -J_{ex}\frac{S(S+1) - S_f(S_f+1) - S_d(S_d+1)}{2}
\end{aligned}
$$
$$(1)$$

Here in eq 1:

$$J_{ex} = 6G^1(fd)/35 + 8G^3(fd)/105 + 20G^5(fd)/231 \quad (2)$$

where $\mathbf{S}_f$ and $\mathbf{S}_d$ are spin operators for the $4f^7$ core and 5d electrons, respectively; $S_f = 7/2$, $S_d = 1/2$, and $S = S_f \pm 1/2$ are the spin quantum numbers for the ^8S multiplet of the $4f^7$ core, 5d electron, and total spin, respectively.

An ab initio calculation of $G^k(fd)$ and other parameters is available[12] but is known to be greatly overestimated.[2] From those values[12] we obtain $J_{ex}(calcd) = 3605\ cm^{-1}$. For Tb^{3+}, the splitting between bands A $(S = 4)$ and B $(S = 3)$ due to eq 1 is then $4J_{ex}$, so we obtain $J_{ex}(expt) = 1925\ cm^{-1} = 0.55 J_{ex}(calcd)$, which is slightly larger than the $0.53\ J_{ex}(calcd)$ for Cs_2NaYCl_6.[9]

Continuing with the analysis of Figure 1, the energy difference between bands E and A is $\sim 34\,300\ cm^{-1}$, which is slightly larger than the $^6P - ^8S$ splitting of Gd^{3+}. Considering that the Coulomb interaction for the $4f^7$ core of Tb^{3+} is larger than that of $4f^8$ Tb^{3+} by about 6%, and that the latter is larger than that of Gd^{3+} by 3.5%,[1] we assign the bands E as $^7[(4f^7\ ^6P)\ t_{2g}]$. Then, the energy differences between F and E, $\sim 3500\ cm^{-1}$, and between G and E, $\sim 7000\ cm^{-1}$, prompt us to assign F and G as $^7[(4f^7\ ^6I)\ t_{2g}]$ and $^7[(4f^7\ ^6D)\ t_{2g}]$. The fine structures are due to further splitting of the "multiplets" by 5d and 4f spin—orbit interactions, as well as to vibronic structure.

The broad features C and D are assigned to SF and SA transitions with terminal states $^{2S+1}[(4f^7\ ^8S)\ e_g]$ (C, $S = 4$; D, $S = 3$), which are broadened by the stronger interaction of e_g orbitals with ligands. Subtraction of their energies gives the LS—HS splitting of $\sim 8000\ cm^{-1}$, which is the same as that derived from the energy difference between B and A. The energy difference between C and A (or between D and B) is around $\Delta E(e_g - t_{2g}) = 21\,600\ cm^{-1}$, which is intermediate between the values 18 200 and 26 800 cm^{-1} given for Ce^{3+} in Rb_2NaYF_6 and Rb_2NaScF_6, respectively.[13] Using the equality $\Delta E(e_g - t_{2g}) = 10B_0^4/21$ for an O_h site, the d-electron fourth-order crystal field parameter is then estimated to be $B_0^4 = 45\,360\ cm^{-1}$ for Tb^{3+} in Cs_2NaYF_6.

Contrary to expectation, the SA transition D is not much stronger than the SF transition C. This observation can be
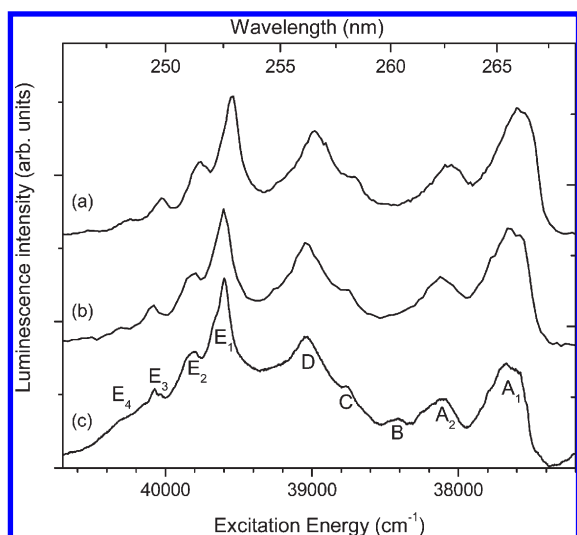
Figure 2. Spectra for the lowest energy $4f^8 \rightarrow 4f^7 5d$ spin-forbidden transitions of Tb^{3+}: (a) excitation spectra measured at 12.6 K by monitoring the 541 nm emission of $Cs_2NaY_{0.99}Tb_{0.01}F_6$, using a slit width of 0.3 nm and scanning with step of 0.1 nm; (b) excitation spectra measured at 10 K by monitoring the 540 nm emission of another crystal of $Cs_2NaY_{0.99}Tb_{0.01}F_6$, using a slit width of 2.5 nm with 0.2 nm steps; (c) ultraviolet absorption spectrum of $Cs_2NaY_{0.9}Tb_{0.1}F_6$ measured at 2.2 K with a slit width of 0.05 nm.

explained by the fact that the spectrum is an excitation spectrum (i.e., not an absorption spectrum) and that the terminal states for D are probably more easily ionized into the conduction band than those for C.

The major features in the spectrum of Figure 1 have thus been rationalized. Now we focus upon the lowest energy SF transition under higher resolution, as depicted in Figure 2. The corresponding absorption spectrum of Cs_2NaYCl_6:Tb^{3+} clearly exhibits only three electronic transitions[9] and each one comprises vibrational progressions in totally symmetric modes. This arises because only three of the eleven LS $4f^7 5d$ crystal field states have the requisite symmetry irreducible representation (T_{1u}) for an ED allowed transition from the $^7F_6 A_{1g}$ ground state. However, it is unclear how the features in Figure 2 can be assigned to only three electronic transitions. One possibility that can be excluded is the observation of coincident $4f^8 \rightarrow 4f^8$ intraconfigurational transitions in this spectral region. Our calculations show that there are 26 $4f^8$ electronic states between 37 500 and 40 300 cm^{-1}. Intraconfigurational transitions of Ln^{3+} are magnetic dipole or vibronically enabled. The pure electronic transitions to T_{1g} states from the $^7F_6$ electronic ground state are expected to manifest sharp features because they are potentially magnetic dipole allowed. However, since the terminal multiplets in this spectral region correspond to ^5I_J ($J = 4, 5, 6$) and $^5K_9$, the transitions are calculated to be very weak in intensity. This is supported by the fact that no weak, sharp bands are apparent in this region. The $4f^8$–$4f^8$ vibronic transitions are also expected to be very weak. We therefore discount the possibility that some of the observed structure between 37 500 and 40 300 cm^{-1} is due to intraconfigurational transitions.

The highest energy SF transitions in Figure 2, labeled E_1–E_4, are the most clearly resolved features, so that we commence the spectral analysis with these bands. The feature E_1 is clearly a new zero phonon line, and it has a shoulder at ~75 cm^{-1} to high energy. By analogy with the Cs_2NaYCl_6:Tb^{3+} spectrum, this may

correspond to a cesium mode, with the energy similar to that of the τ_{2g} Raman-active vibration. Furthermore, the band E_3 corresponds to the first member of the totally symmetric $\nu_1 \alpha_{1g}$ TbF_6^{3-} moiety stretching mode upon the electronic origin, with the derived frequency of 475 cm^{-1}. The band E_2 (and its subsequent ν_1 progression member, E_4) are then unassigned and either correspond to a new electronic transition or to another vibrational progression in a mode of 201 ± 10 cm^{-1}. We are unable to offer an explanation to justify the former assumption, whereas the latter one is possible if a first-order linear Jahn–Teller effect is operative in the t_{2g} orbital. The term linear denotes that the effect is linear to vibrational normal coordinates, whereas first-order means that the electronic part of the matrix elements of the linear term between the otherwise degenerate t_{2g} orbital are nonzero and hence split t_{2g} directly. The criterion for this to happen is in fact fulfilled because the symmetric direct product $[t_{2g} \times t_{2g}]$ contains the symmetry irreducible representations $T_{2g} + E_g$. From the Raman spectrum, the ground-state vibrational frequencies of the τ_{2g} and ε_g modes are 194 and 362 cm^{-1}, respectively. We conclude that a Jahn–Teller effect in the τ_{2g} mode is operative which effectively reduces the site symmetry from O_h to D_{4h} or even D_{2h}. Jahn–Teller effects concerning t_{2g} orbitals have been well-studied for intraconfigurational transitions of 3d-electron systems, where the spin–orbit coupling is much weaker than in the present scenario.[14−16] In those cases it was generally expected that interactions with τ_{2g} vibrations could be neglected since these involve tangential motion in the MX_6 octahedron and couple to π- rather than σ-bonding orbitals. A major difference of Jahn–Teller interaction in the present 4f–5d interconfigurational transition is the switching of a forbidden transition in O_h symmetry to an ED allowed one due to the D_{4h} (or even D_{2h}) perturbation, as discussed below.

The lowest energy SF transition exhibits broad structure in Figure 2, with the 0–0 transition (A_1) and its ν_1 phonon replica (A_2) at ~470 cm^{-1} to higher energy. The features C, D (in addition to the weak band B in the absorption spectrum) remain to be assigned, but it is not possible to identify the separations of these bands as only one electronic transition when using the vibrational frequencies of TbF_6^{3-}. The separations between the zero-phonon lines of the corresponding SF transitions in $Cs_2NaY_{1-x}Tb_xCl_6$ are 650 cm^{-1} (I−II) and 608 cm^{-1} (II−III). From the analysis given for the SF transition of Tb^{3+} in the latter system,[9] the splitting of the lowest three observed T_{1u} levels is caused by the spin–orbit interaction of the 5d electron, and the derived spin–orbit constant $\zeta_{5d}(Cl)$ in that case was 1185 cm^{-1}. Under the assumption that the corresponding separations (A_1−B and B−E_1) for $Cs_2NaY_{1-x}Tb_xF_6$ are also solely due to 5d spin–orbit interaction, the parameter $\zeta_{5d}(F)$ would then be >2000 cm^{-1}. This value is considered unlikely when compared with the ab initio (1557 cm^{-1}) and free-ion (1389 cm^{-1}) values.[12]

The effective symmetry reduction from O_h to D_{4h} (or D_{2h}) would mix T_{1u} character into $T_{2u}(O_h)$ states, so that new 4f–5d SF transitions are then possible. Such a distortion can be treated by introducing crystal-field interactions of symmetry lower than O_h. Since the measured spectrum (Figure 2) is composed not only of zero-phonon lines (which can be calculated from a diagonalization of the crystal field empirical Hamiltonian) but also of vibronic peaks, a realistic calculation to precisely simulate the interplay of the distortion and vibronic bands cannot be made herein. As a preliminary alternative, the calculated effects of a tetragonal distortion upon the SF transition of Tb^{3+} in $Cs_2NaY_{1-x}Tb_xF_6$ are displayed in Figure 3a,b for various values of B_0^2 and B_2^2,
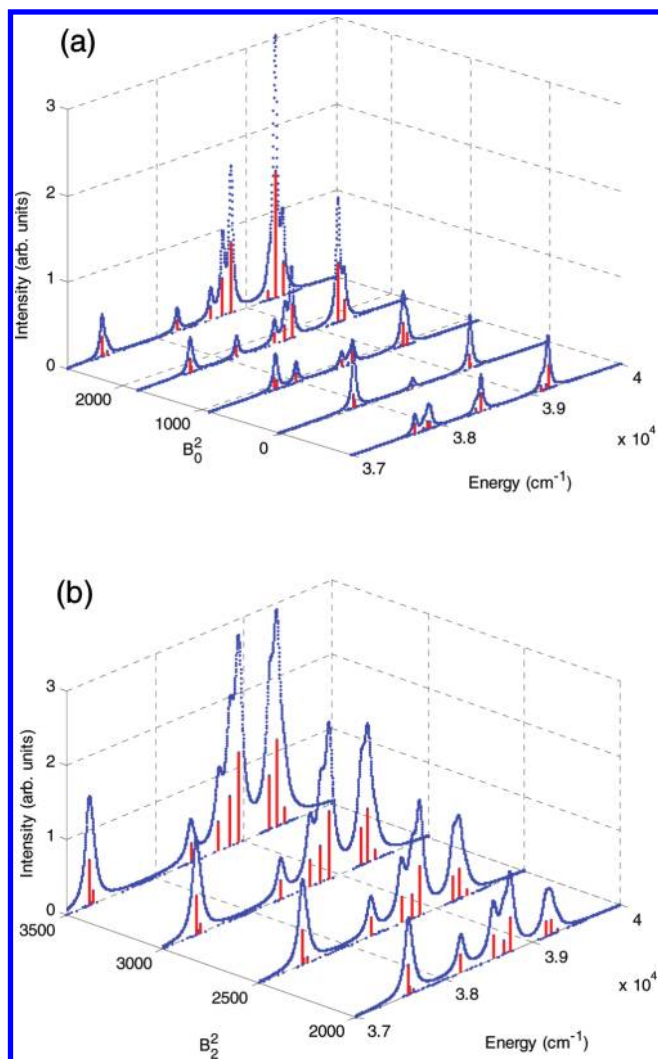
Figure 3. Calculated zero-phonon lines and their convolutions (using a Gaussian function with standard deviation of 100 cm^{-1}) for the lowest energy SF transition of Tb^{3+} in Cs$_2$NaY$_{1-x}$Tb$_x$F$_6$ when distortion is included with 5d crystal-field interactions: (a) B_0^2; (b) B_2^2.

Tb—F bond distance of ~2.28 Å.[17] For the highest energy SF transition, the distortion along the τ_{2g} coordinate is 0.08 ± 0.01 Å, which corresponds to the rather small Jahn—Teller stabilization energy of ~75 cm^{-1}.

CONCLUSIONS

Jahn—Teller interactions have seldom been reported for lanthanide complexes. From the occurrence of large Stokes shifts in emission spectra, Andriessen et al.[18] inferred the operation of a pseudo-Jahn—Teller effect in the 5d states of Ce^{3+} in several host lattices. We previously considered a linear Jahn—Teller effect from the tentative observation of vibrational progressions in the τ_{2g} mode for the SF transition of Tb^{3+} in Cs$_2$NaY$_{1-x}$Tb$_x$Cl$_6$,[9] but the present results are more conclusive.

AUTHOR INFORMATION

Corresponding Author
*E-mail: bhtan@cityu.edu.hk. Fax: 852 3442 0522. Phone: 852 3442 7840.

REFERENCES

(1) Duan, C.-K.; Tanner, P. A. *J. Phys. Chem. A* **2010**, *114*, 6055.
(2) van Pieterson, L.; Reid, M. F.; Burdick, G. W.; Meijerink, A. *Phys. Rev. B* **2002**, *65*, 045114.
(3) Wegh, R. T.; Meijerink, A. *Phys. Rev. B* **1999**, *60*, 10820.
(4) van Pieterson, L.; Reid, M. F.; Meijerink, A. *Phys. Rev. Lett.* **2002**, *88*, 067405.
(5) Tanner, P. A.; Duan, C.-K.; Makhov, V. N.; Kirm, M.; Khaidukov, N. M. *J. Phys.: Condens. Matter* **2009**, *21*, 395504(The sharp bands between 120 and 140 nm were associated with the 5d component e$_g$, but this typographical error is corrected herein as t$_{2g}$).
(6) van Pieterson, L.; Reid, M. F.; Wegh, R. T.; Soverna, S.; Meijerink, A. *Phys. Rev. B* **2002**, *65*, 045113.
(7) Barandiarán, Z.; Seijo, L. *Theor. Chem. Acc.* **2006**, *116*, 505.
(8) Ruipérez, F.; Barandiarán, Z.; Seijo, L. *J. Chem. Phys.* **2005**, *123*, 244703.
(9) Ning, L.; Mak, C. S. K.; Tanner, P. A. *Phys. Rev. B* **2005**, *72*, 085127.
(10) Duan, C. -K.; Tanner, P. A.; Babin, V.; Meijerink, A. *J. Phys. Chem. C* **2009**, *113*, 12580.
(11) Berry, A. J.; Morrison, I. D.; Denning, R. G. *Mol. Phys.* **1998**, *93*, 1.
(12) Reid, M. F.; van Pieterson, L.; Meijerink, A. *J. Alloys Compd.* **2002**, *344*, 240.
(13) Aull, B. F.; Jenssen, H. P. *Phys. Rev. B* **1986**, *34*, 6647.
(14) Wilson, R. B.; Solomon, E. I. *Inorg. Chem.* **1978**, *17*, 1729.
(15) Sturge, M. D. *Phys. Rev. B* **1970**, *1*, 1005.
(16) Wenger, O. S.; Güdel, H. U. *J. Chem. Phys.* **2001**, *114*, 5832.
(17) Meyer, G. *Progr. Solid State Chem.* **1982**, *14*, 141.
(18) Andriessen, J.; van der Kolk, E.; Dorenbos, P. *Phys. Rev. B* **2007**, *76*, 075124.

respectively. In this figure, the 5d spin—orbit interaction has been taken (1200 cm^{-1}) as intermediate between the values for the free-ion and Tb^{3+} in Cs$_2$NaY$_{1-x}$Tb$_x$Cl$_6$. Note that the actual distortion may require more than these two additional crystal-field parameters and that no vibronic structure has been included in the simulations. The simulations exhibit complexity and increased intensity in the middle region (38 000−39 000 cm^{-1}) of the SF transitions. It is evident that if only B_0^2 (or B_2^2) is important, the best value to describe the experimental data is 2000 (3000) cm^{-1}. In these two cases the spread of the total splitting of the SF transitions increases from ~1300 cm^{-1} (when $B_0^2 = 0$ and $B_2^2 = 0$) to ~2000 cm^{-1} (when either $B_0^2 = 2000$ cm^{-1} or $B_2^2 = 3000$ cm^{-1}). Such values are small compared to B_0^4 and are actually a small distortion on top of the octahedral arrangement of ligands.

The distortion in the totally symmetric vibrational coordinate, as estimated from the intensity of the first member of the ν_1 progression, is 0.1 Å for the terminal state of the lowest energy SF transition and 0.04 ± 0.02 Å for that of the highest energy SF transition. These distortions are small when compared with the

9191

dx.doi.org/10.1021/jp205011v |*J. Phys. Chem. A* 2011, 115, 9188–9191